Physics – Uspekhi **66** (9) 936 – 942 (2023)

INSTRUMENTS AND METHODS OF INVESTIGATION PACS numbers: **61.46. – w, 61.48. – c, 68.43. – h, 89.30. – g**

Method of thermal desorption study of hydrogen states in carbon materials and nanomaterials

Yu S Nechaev, E A Denisov, A O Cheretaeva, N A Shurygina, E K Kostikova, S Yu Davydov

DOI: https://doi.org/10.3367/UFNe.2022.11.039274

Contents

Abstract. An efficient technique for processing, analyzing, and interpreting thermal desorption spectra (TDSs) of hydrogen in carbon materials and nanomaterials obtained using a single heating rate is developed, which makes it possible to study various states of hydrogen and determine the characteristics corresponding to them, including the rate constants and activation energies of desorption processes. The method is no less informative, but much less laborious from the experimental point of view, than the generally accepted (to determine such characteristics) Kissinger method, which requires using several heating rates and has strict limits on applicability. The developed technique is based on approximating the hydrogen TDS by Gaussians and processing their peaks in the approximation of first and second order reactions. The technique includes the use of nonstandard criteria of 'likelihood' and/or 'physicality' of the results, as well as verification and/or refinement of the results by numerical modeling methods that allow approximating TDSs not by Gaussians but by curves corresponding to first or second order reactions.

Keywords: carbon materials and nanomaterials, method of desorption study of hydrogen states, approximation of desorption spectra by Gaussians and non-Gaussians, approximations of first and second order reactions, characteristics of desorption processes

Yu S Nechaev [1, a], **E A Denisov** [2, b], **A O Cheretaeva** [3, c], **N A Shurygina** [1, d], **E K Kostikova** [4, e], **S Yu Davydov** [5, f]
[1] I P Bardin Central Research Institute for Ferrous Metallurgy, Scientific Center of Metals Science and Physics, ul. Radio 23/9, str. 2, 105005 Moscow, Russian Federation
[2] St. Petersburg State University, Universitetskaya naberezhnaya 7/9, 199034 St. Petersburg, Russian Federation
[3] Togliatti State University, Research Institute of Progressive Technologies, ul. Belorusskaya 14, 445020 Togliatti, Russian Federation
[4] Institute of Applied Mathematical Research, Karelian Research Centre, Russian Academy of Sciences, ul. Pushkinskaya 11, 185910 Petrozavodsk, Russian Federation
[5] Ioffe Institute, Russian Academy of Sciences, ul. Politekhnicheskaya 26, 194021 St. Petersburg, Russian Federation
E-mail: [a] yuri1939@inbox.ru, [b] denisov70@bk.ru, [c] a.cheretaeva@tltsu.ru, [d] shnadya@yandex.ru, [e] fedorova@krc.karelia.ru, [f] sergei_davydov@mail.ru

Received 4 March 2022, revised 12 November 2022
Uspekhi Fizicheskikh Nauk **193** (9) 994 – 1000 (2023)
Translated by V L Derbov

1. Introduction

The problem of studying in detail the states and characteristics of hydrogen in carbon nanostructures and graphite is urgent in connection with the impact of hydrogen on the physical properties of these functional and constructional materials [1–4].

A generally accepted method for determining the main characteristics of hydrogen (activation energies and desorption rate constants) is thermal desorption spectroscopy (TDS) of hydrogen using several rates of material linear heating, the so-called Kissinger method [5]. However, in addition to high labor consumption, this method is characterized by severe limitations on its applicability, noted in Refs [4, 6, 7]. Therefore, the overwhelming majority of known TDS studies are carried out using a single heating rate of the material and without determining the rate constants of desorption processes. As noted in many publications (see, e.g., [4, 6–9]), in this case there are difficulties with processing, approximating, and interpreting TDS data, which is the cause of the main gaps in knowledge in the field. It should be noted that in many studies only the first-order reaction approximation was used to process thermodesorption spectra, whereas in other studies only the second-order reaction approximation was used. It should also be noted that there is a big difference between and large scatter in the experimental and theoretical values of the characteristics of hydrogen desorption processes in such materials.

For these reasons, it seems appropriate to develop an effective technique for the thermodesorption study (using a single rate of material heating) of the states and characteristics of hydrogen and to apply this technique to the analysis and interpretation of a number of known and the most representative experimental TDS data for hydrogen in carbon materials and nanomaterials.

The present methodological study takes into account all the above issues. The aims and objectives of our study include considering an efficient technique [10–14] of thermodesorption study of hydrogen states and the results of its application [12–21] to a number of experimental TDS data (including those obtained with a single heating rate) for carbon materials and nanomaterials. The results of applying approximations of both first-order and the second-order reactions to desorption processes are considered and compared.

2. Techniques for processing and analyzing thermodesorption spectra of hydrogen

The technique [10–21] developed and applied to solve the problem [1–4] formulated in the Introduction allows determining the activation energies Q and pre-exponential factors K_0 of rate constants K of desorption processes that correspond to desorption peaks with different temperatures ($T_{\max}$) of the maximal desorption rate from the TDS recorded using a single heating rate β of material, as shown in Sections 3–6. A number of other studies, in particular [6–9, 22, 23], were taken into account when developing this technique.

The method [12] comprises several stages of realization, including the use of nonstandard criteria of 'likelihood' and/or 'physicality' of the results, as well as verification and/or refinement of the results by numerical modeling methods [14].

The first stage consists in approximating the studied spectrum by Gaussians, the number of which varies and is in some sense optimized to obtain the most 'physical' results. The second stage consists in determining the rate constant $K(T)$ of hydrogen desorption at various temperatures, close to $T_{\max}$, in the first-order reaction approximation for each Gaussian (from the temperature dependence of the desorption rate $-\mathrm{d}\theta/\mathrm{d}t$ divided by β), whence the values of Q and K_0 are determined (using the Arrhenius equation). In this case, the kinetic equation for the first-order reaction is used in the form

$$-\frac{1}{\beta}\frac{\mathrm{d}\theta}{\mathrm{d}t} = -\frac{\mathrm{d}\theta}{\mathrm{d}T} = K\frac{\theta}{\beta} = K_0\left(\frac{\theta}{\beta}\right)\exp\left(-\frac{Q}{RT}\right), \qquad (1)$$

where t is the time, T is the absolute temperature, R is the universal gas constant, $\theta = C/C_0$ is the relative average concentration of hydrogen in the sample, corresponding to the considered Gaussian (for given values of T and t), and $\theta = 1$ at $t = 0$.

The criterion of 'likeliness' (Q^*) for the obtained values of the desorption activation energy Q, showing the correspondence (at $Q^* \approx Q$) to the Kissinger model [5, 10], can be obtained from the condition of maximum desorption rate ($\mathrm{d}^2\theta/\mathrm{d}T^2 = 0$) in the form

$$Q^* \approx \frac{RT_{\max}^2 K(T_{\max})}{\beta}, \qquad (2)$$

where the values of $T_{\max}$ and $K(T_{\max})$ can be taken (in a satisfactory approximation) from the above results for the considered Gaussian.

The next stage consists in determining the values of Q and K_0 in the approximation of the second-order reaction for each of the Gaussians. In this case, the following kinetic equation for a second-order reaction is used:

$$-\frac{1}{\beta}\frac{\mathrm{d}\theta}{\mathrm{d}t} = -\frac{\mathrm{d}\theta}{\mathrm{d}T} = K\frac{\theta^2}{\beta} = K_0\left(\frac{\theta^2}{\beta}\right)\exp\left(-\frac{Q}{RT}\right). \qquad (3)$$

The likeliness criterion Q^* can be obtained from the condition $\mathrm{d}^2\theta/\mathrm{d}T^2 = 0$ in the form

$$Q^* \approx \frac{2RT_{\max}^2\theta(T_{\max})K(T_{\max})}{\beta}, \qquad (4)$$

where the value of $\theta(T_{\max})$ can be taken equal to 0.5 (with an error of about 15%).

The next stage consists in refining (and/or confirming) the results obtained above (using approximations of both the first-order and the second-order reaction) by means of numerical simulation [14] of the desorption spectra. It should be noted that, in this case, the considered spectra are approximated by peaks, corresponding to processes of the first or second order, rather than by Gaussians; the error (and/or scatter) in the determination of the values of Q and $\ln K_0$ in most cases amounts to $\sim 15\%$.

The final stage is considering the issue of the 'physicality' of the obtained results and their interpretation.

The efficiency of the described technique is confirmed by the recently published results of its application to hydrogen thermodesorption studies in a number of carbon nanostructures and graphite materials (see Sections 3–6).

3. Thermodesorption spectra of hydrogen in graphite materials

In Ref. [24], using the method of thermodesorption spectroscopy, the interaction of atomic hydrogen with pyrolitic graphite with a density of 2.19 g cm^{-3} was studied. The samples were exposed (for 2 hours) to atomic hydrogen (at a pressure of ~ 1 Pa and temperature of 873 K). In the thermodesorption spectra recorded using three heating rates (25, 10, and 100 K s^{-1}), only two major (self-manifesting) peaks were considered [24].

The results of a more detailed processing and analysis (methods [12, 14]) of the TDS data [24] for pyrolitic graphite (six thermodesorption Gaussian peaks) are presented in Fig. 1 and Table 1; they are also described in Ref. [21]. Note that the approximation of this spectrum by exactly six Gaussians is based on the obtained dependence of the quadratic parameter of the agreement between the theoretical curve and the experimental one on the number of Gaussians (see the inset in Fig. 1). The characteristics of all six Gaussians, including those corresponding to two major peaks mentioned above (*2* and *6*), are presented in Table 1.

Analysis shows that one of the two major peaks in Fig. 1 (peak *2*) corresponds to a reaction of the first order with the following characteristics: $Q_2 \approx 201$ kJ mol^{-1}, $K_{02} \approx 7.3\times 10^8$ s^{-1} (see Table 1). The process can be limited by hydrogen diffusion with a 'reversible' capture of the diffusant by the chemosorption 'traps' described in Refs [10, 11], freely accessible on the Internet, for the diffusion processes denoted in the above papers as type III processes. The characteristic diffusion length for the process corresponding to peak *2* can be estimated (according to [10, 11, 21]) as $L_2 \approx (D_{0\mathrm{III}[10]}/K_{02})^{1/2} \approx$

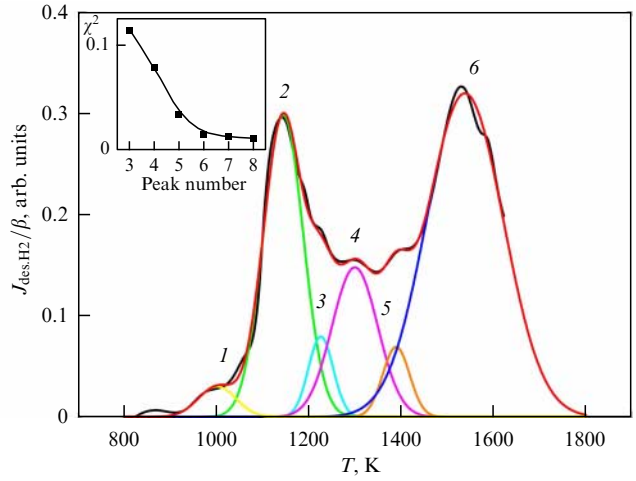

Figure 1. Approximation by Gaussians (method of [12, 14]) of the thermodesorption spectrum ($\beta = 25$ K s^{-1}) of hydrogen for pyrolitic graphite [24] exposed to atomic hydrogen (2 hours at a pressure of ~ 1 Pa and temperature of 873 K). Inset shows dependence of the quadratic parameter of the correspondence of the theoretical curve to the experimental one on the number of Gaussians.

6×10^{-6} cm, where $D_{0III[10]} \approx 3 \times 10^{-3}$ cm^2 s^{-1} is the pre-exponential factor of the effective hydrogen diffusion coefficient for type III processes [10].

Analysis also shows that the second major peak (peak *6* in Fig. 1) corresponds to a reaction of the second order with the characteristics $Q_6 \approx 377$ kJ mol^{-1}, $K_{06} \approx 3 \times 10^{12}$ s^{-1} (see Table 1). In this case, the reaction can be limited by processes of recombination of hydrogen atoms into molecules and desorption of these atoms from so-called reversible chemosorption hydrogen traps (models G and/or F in Refs [10, 11]) on the free surface of the sample, which is described by the Polanyi–Wigner equation for second-order reactions [10].

In a similar way, we can consider the remaining four Gaussians (relatively small peaks *1* and *3–5*).

The results of the detailed processing and analysis (methods [12, 14]) of the data [4, 25–28] on hydrogen thermodesorption from various graphite materials, hydrated in gaseous atomic or molecular hydrogen, are presented in Refs [15, 16, 21].

4. Thermodesorption spectra of hydrogen in graphene structures

Reference [29] investigates the phase transition induced by hydrogen adsorption in epitaxial graphene containing from one to four hydrogen-saturated (in gaseous atomic hydrogen) graphene layers on a substrate of Pt (111) to a diamond-like structure close to that of graphane [30, 31]. Several up-to-date research methods were applied, including thermodesorption spectroscopy. However, the authors of [29] hardly processed the TDS data obtained by them using a single rate of heating.

The results of processing and analysis (methods [12, 14]) of the TDS data [29] for such epitaxial graphene with a graphane-like structure and a certain content of chemosorbed hydrogen are presented in Fig. 2a, b and Table 2. The physics of processes corresponding to four studied thermodesorption peaks (states) is described in detail in Ref. [12].

Note that the found characteristics (see Table 2) of peak *4* in Fig. 2a ($Q_4 \approx 224$ kJ mol^{-1}, $K_{04} \approx 1.4 \times 10^{15}$ s^{-1}) and in Fig. 2b ($Q_4 \approx 228$ kJ mol^{-1}, $K_{04} \approx 2.6 \times 10^{15}$ s^{-1}) are close to the theoretical [30] and experimental [31] values of the energy of separation of a hydrogen atom from graphane and the frequency of hydrogen atom oscillation in graphane, respectively, considered in Refs [11, 12].

The results of a detailed processing and analysis (methods [12, 14]) of data [22] on the thermodesorption of hydrogen from graphene sheets hydrated in plasma are presented in Ref. [12].

Table 1. Results of processing and analysis (methods [12, 14]) of six Gaussians* (peaks *1–6* in Fig. 1) in the approximation of first-order and second-order reactions.

Peak No.	T_{max}, K	Order of reaction	Q, kJ mol^{-1}	K_0, s^{-1}	$K(T_{max})$, s^{-1}	Q^*, kJ mol^{-1}	γ	C_0
1	1001	First	163	1.5×10^8	0.47	162	0.02	5.0×10^{-9}
		Second	326	1.0×10^{17}	0.97	325		
2	1145	First	201	7.3×10^8	0.49	201	0.25	6.2×10^{-8}
		Second	402	2.2×10^{18}	1.00	401		
3	1226	First	373	5.7×10^{15}	0.73	371	0.04	1.0×10^{-8}
		Second	745	8.6×10^{31}	1.50	742		
4	1300	First	227	5.3×10^8	0.40	225	0.14	3.5×10^{-8}
		Second	452	1.2×10^{18}	0.82	451		
5	1389	First	441	2.6×10^{16}	0.68	437	0.04	1.0×10^{-8}
		Second	876	1.2×10^{33}	1.40	874		
6	1538	First	189	6.3×10^5	0.24	188	0.51	1.3×10^{-7}
		Second	377	3.0×10^{12}	0.47	376		

* γ is the fraction in the spectrum, $C_0 = \gamma[H/C]_{\Sigma vol.}$ is the initial atomic fraction of hydrogen in the sample corresponding to a given peak, $[H/C]_{\Sigma vol.} \sim 2.5 \times 10^{-7}$ is the total initial atomic fraction of hydrogen in the sample.

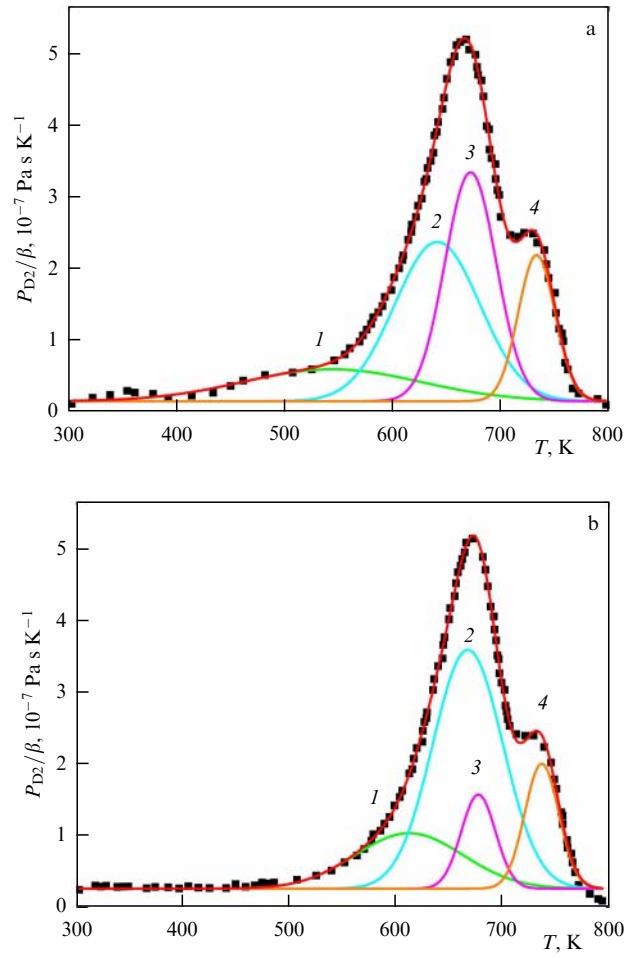

Figure 2. Processing (methods [12, 14]) of thermodesorption spectra ($\beta = 3$ K s^{-1}) ([29], Fig. 1) of deuterium for hydrogen-saturated graphene layers with a diamond-like structure on a Pt(111) substrate. Approximation by four Gaussians of the spectrum (a) for single-layer (H-SLG) epitaxial graphene and (b) for four-layer (H-FLG) epitaxial graphene.

5. Thermodesorption spectra of hydrogen in carbon nanotubes

The results of processing and analyzing TDS data [32] on the physical sorption of hydrogen in single-wall carbon nanotubes (SWCNTs) hydrated in gaseous molecular hydrogen are presented in Fig. 3 and Table 3.

The values (see Table 3) of the desorption activation energy Q and the pre-exponential factor of the rate constant K_0 obtained for five self-manifesting desorption peaks (see Fig. 3) are apparently related to the processes of physical adsorption of hydrogen by carbon nanostructures [10, 33], which can be approximated as reactions of the first order.

6. Thermodesorption spectra of hydrogen in graphite nanofibers

The results of processing and analyzing (using the methods of [12, 14]) the thermodesorption spectrum for the 'irreversible' hydrogen in graphite nanofibers (GNFs) [34], hydrated in gaseous molecular hydrogen, are presented in Fig. 4a and Table 4, as well as in Refs [18–20]. Note that the total (specified) content of 'irreversible' hydrogen in GNF samples ($C_{H2\Sigma} \approx 11 \pm 3$ wt.%) was determined from data from Refs [34, 35].

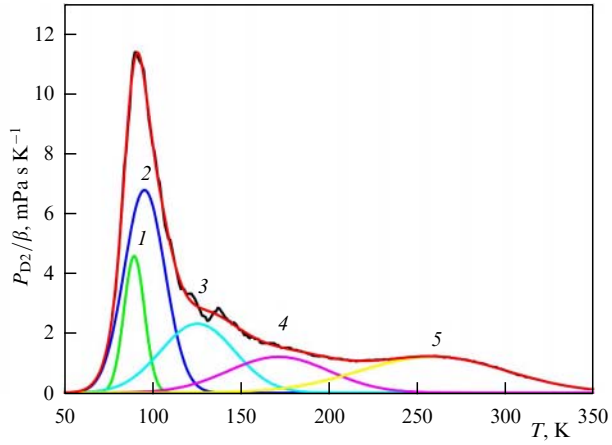

Figure 3. Approximation by five Gaussians (peaks *1–5*) of the deuterium thermodesorption spectrum (Fig. 1 in Ref. [32], $\beta = 0.067$ K s^{-1}) for a sample of single-wall carbon nanotubes after exposure (1 hour at a temperature of 298 K) to gaseous D_2 at a pressure of 2 MPa. Residual gas was pumped out at 77 K. Red curve shows the sum of five Gaussians, black curve shows the initial experimental spectrum.

The results of processing and analyzing (by methods of [12, 14]) the thermogravimetric (TG) spectrum from Ref. [34] are presented in Fig. 4b and Table 5, as well as in Refs [18–20]. There are reasons to believe that peak *3* in Fig. 4b is mainly due to the gasification of carbon atoms and/or oxygen-containing functional complexes (groups). In this case, it should be taken into account that in Ref. [34] no hydrocarbon products were detected when heating the material in an inert atmosphere at temperatures up to 1300 K. Therefore, the atomic ratio value (H/C) for peak *3* (in Fig. 4b) can be negligibly small, and there is no necessity to approximate this peak with more accuracy.

On the other hand, a significant level of noise for the spectrum in Fig. 4b does not hinder determining the characteristics of the major hydrogen peak *1* (Fig. 4b) with the accuracy required (to achieve the goal of Refs [18–20]).

An analysis [18–20] of the results (see Tables 4 and 5) for the main process of 'irreversible' hydrogen desorption (peak *1* in Fig. 4a and b) from GNF samples [34] shows that a first-order process (reaction) occurs with the following characteristics: $T_{max} = 914-923$ K, $Q \approx 40$ kJ mol^{-1}, $K_0 \approx 2\times 10^{-1}$ s^{-1}, $C_{H2\Sigma} \approx 8$ wt.% (i.e., the atomic ratio is [H/C] ≈ 1). The analysis [18–20] also shows that the desorption process is limited by the hydrogen diffusion accompanied by the 'reversible' capture [6–11] of the diffusant by certain 'centers' of hydrogen chemosorption in GNFs. This is comparable to type I and II diffusion processes (having the activation energies $Q_I \approx 20$ kJ mol^{-1} and $Q_{II} \approx 120$ kJ mol^{-1}, respectively), considered in Refs [10, 11]. The obtained activation energy of desorption $Q \approx 40$ kJ mol^{-1} (see Tables 4 and 5) is (like the above values of Q_I and Q_{II}) an effective activation energy of such diffusion close (in absolute value) to the energy of the diffusant binding to the corresponding 'centers' of chemosorption in the carbon material, which is also considered in Refs [10, 11]. Obviously, such 'centers' are localized between the base carbon planes in the GNF [34]; in this case, they are almost completely filled with hydrogen, i.e., the base carbon planes are, as it were, separated by layers of chemisorbed hydrogen.

The characteristic diffusion length (L) for the considered process, corresponding to peak *1*, can be described (to an order of magnitude) by means of the known [6, 10] expression

Table 2. Results of processing and analyzing (methods [12, 14]) four Gaussians (peaks *1–4* in Fig. 2a and b) for hydrogen-saturated graphene layers on a Pt(111) substrate in the approximation of first-order and second-order reactions.

Peak	T_{max}, K	Order of reaction	Q, kJ mol^{-1}	K_0, s^{-1}	$K(T_{max})$, s^{-1}	Q^*, kJ mol^{-1}	γ
Fig. 2a (H-SLG)							
1	543	First	24	8.8×10^{0}	3.9×10^{-2}	32	0.15
		Second	48	3.4×10^{3}	7.9×10^{-2}	64	
2	640	First	72	5.1×10^{4}	6.4×10^{-2}	72	0.40
		Second	132	7.5×10^{9}	1.3×10^{-1}	144	
3	671	First	130	1.3×10^{9}	1.0×10^{-1}	129	0.30
		Second	252	9.2×10^{18}	2.0×10^{-1}	255	
4	733	First	224	1.4×10^{15}	1.5×10^{-1}	222	0.15
		Second	412	7.8×10^{28}	3.0×10^{-1}	442	
Fig. 2b (H-FLG)							
1	610	First	50	1.1×10^{3}	6.1×10^{-2}	63	0.20
		Second	98	3.2×10^{7}	1.2×10^{-1}	122	
2	665	First	92	1.2×10^{6}	7.5×10^{-2}	92	0.55
		Second	180	2.0×10^{13}	1.4×10^{-1}	177	
3	675	First	193	1.3×10^{14}	1.6×10^{-1}	207	0.11
		Second	377	4.4×10^{28}	3.0×10^{-1}	382	
4	735	First	228	2.6×10^{15}	1.6×10^{-1}	242	0.14
		Second	456	8.6×10^{31}	3.1×10^{-1}	457	

Table 3. Results of processing and analyzing (methods [12, 14]) five peaks shown in Fig. 3 for single-wall carbon nanotubes in the approximation of first-order processes.

Peak	T_{max}, K	Q, kJ mol^{-1}	K_0, s^{-1}	$K(T_{max})$, s^{-1}	Q^*, kJ mol^{-1}	γ	Wt. %	[D/C]
1	90	9.2	2.1×10^{3}	9.1×10^{-3}	9.1	0.11	0.13	0.008
2	95	5.3	3.5×10^{0}	4.6×10^{-3}	5.2	0.33	0.40	0.024
3	126	5.0	3.0×10^{-1}	2.5×10^{-3}	5.0	0.20	0.24	0.014
4	172	6.8	2.2×10^{-1}	1.9×10^{-3}	6.8	0.14	0.17	0.010
5	259	10.7	1.8×10^{-1}	1.3×10^{-3}	10.7	0.21	0.25	0.015

Table 4. Results of processing and analyzing (methods [12, 14]) three peaks* (Fig. 4a) in the approximation of first-order and second-order reactions (from Refs [34, 35]).

Peak	T_{max}, K	Order of reaction	Q, kJ mol^{-1}	K_0, s^{-1}	$K(T_{max})$, s^{-1}	Q^*, kJ mol^{-1}	γ	C_{H2}, wt. %	[H/C]
1	914	First	39	1.5×10^{-1}	9×10^{-4}	39	0.76	8.4	1.1
		Second	77.5	5.1×10^{1}	2×10^{-3}	77.5			
2	1036	First	199	4.2×10^{7}	4×10^{-3}	198	0.02	0.2	0.02
		Second	398	8.8×10^{17}	7×10^{-3}	396			
3	1161	First	126	8.5×10^{2}	2×10^{-3}	125	0.22	2.4	0.30
		Second	250	7.0×10^{8}	4×10^{-3}	250			
* [H/C] — atomic ratio (hydrogen/carbon) corresponding to the weight content of hydrogen ($C_{H2} = \gamma C_{H2\Sigma}$) for a given peak, $C_{H2\Sigma} \approx 11 \pm 3$ wt.%.									

$L \approx (D_0/K_0)^{1/2}$, where $K_0 \approx 0.15$ s^{-1} (see Table 1). Setting $L \approx L_{sample} \approx 1$ cm, which corresponds to a definite size of the sample [34] (a bundle of graphite nanofibers), we get $D_0 \approx 5$ cm^2 s^{-1} (at $Q \approx 40$ kJ mol^{-1} (see Table 1)), comparable to the characteristics (D_0 and Q) for type I and II processes [10, 11].

Table 5. Results of processing and analyzing (methods [12, 14]) three peaks* (Fig. 4b) in the approximation of first-order and second-order reactions.

Peak	T_{max}, K	Order of reaction	Q, kJ mol^{-1}	K_0, s^{-1}	$K(T_{max})$, s^{-1}	Q^*, kJ mol^{-1}	γ	Wt. %	[H/C]
1	923	First	43	2.9×10^{-1}	1×10^{-3}	43	0.23	8.5	1.1
		Second	87	1.7×10^{2}	2×10^{-3}	87			
2	1165	First	152	1.5×10^{4}	2×10^{-3}	152	0.08	2.9	0.4
		Second	304	2.0×10^{11}	4×10^{-3}	303			
3	1345	First	149	1.0×10^{3}	2×10^{-3}	148	0.69	26	
		Second	298	1.2×10^{9}	1×10^{-2}	297			

*γ is the fraction of the peak in the spectrum, [H/C] is the atomic ratio (hydrogen/carbon) corresponding to the hydrogen content (in wt.%) for a given hydrogen peak obtained by appropriate integration of this peak.

In a similar way, it is also possible to consider in [18–20] the processing results (see Tables 4 and 5) for the remaining (less significant) desorption peaks in Fig. 4a, b.

Reference [17] presents the results of processing and analyzing in detail (method [12, 14]) thermodesorption and other data [36] for graphite nanofibers subjected to hydration in H_2 at a pressure of 9 GPa and temperature of 753 K (with subsequent quenching). This procedure led to a total hydrogen content of up to 6.3 wt. % and a manifestation of three different states of hydrogen, corresponding to physical sorption, chemosorption, and high-density molecular hydrogen localized in the closed nanocavities of the material.

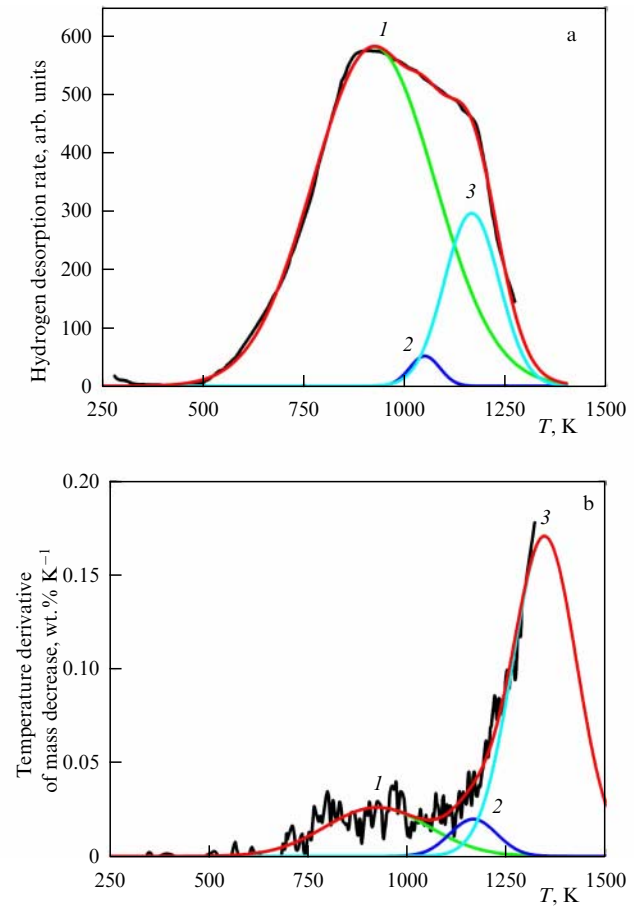

Figure 4. Processing (using the methods of [12, 14]) of data from Ref. [34] for 'super-desorption' of 'irreversible' hydrogen from GNF samples with a herringbone structure (see Fig. 2 in Ref. [34]). Approximation by three Gaussians (peaks *1–3*) of (a) the thermodesorption spectrum (β = 0.17 K s^{-1}) for samples subjected to hydration in gaseous H_2 (at 300 K, 11–4 MPa, 24 h); (b) temperature derivative of the thermogravimetric spectrum for samples subjected to hydration in gaseous H_2 (at 300 K, 11–4 MPa, 24 h) with subsequent heating (β = 0.17 K s^{-1}) in He. Red curves correspond to the sum of three peaks.

The research results discussed in this section are of interest for solving the problem of creating materials and technologies for highly efficient hydrogen storage [2, 37–39] to be used in environmentally friendly road transport.

7. Conclusion

An efficient technique of processing, analyzing, and interpreting thermodesorption spectra of hydrogen in carbon materials and nanomaterials recorded at a single heating rate is developed. The technique allows studying various states of hydrogen and determining the corresponding characteristics, including rate constants and activation energies of desorption processes. The efficiency of the proposed technique is confirmed by recently published results of hydrogen thermodesorption studies in a number of carbon nanostructures and graphite materials considered in the present paper.

This study was carried out with financial support from the Russian Foundation for Basic Research, project no. 18-29-19149 mk.

References

1. Hou J et al. *Phys. Chem. Chem. Phys.* **13** 15384 (2011)
2. Tozzini V, Pellegrini V *Phys. Chem. Chem. Phys.* **15** 80 (2013)
3. Tanabe T *Plasma Phys. Rep.* **45** 300 (2019); *Fiz. Plazmy* **45** 387 (2019)
4. Atsumi H, Kondo Y *Fusion Eng. Design* **131** 49 (2018)
5. Kissinger H E *Anal. Chem.* **29** 1702 (1957)
6. Wei F-G, Enomoto M, Tsuzaki K *Comput. Mater. Sci.* **51** 322 (2012)
7. Drexler A et al. *Int. J. Hydrogen Energy* **46** 39590 (2021)
8. Legrand E et al. *Int. J. Hydrogen Energy* **40** 2871 (2015)
9. Ebihara K et al. *ISIJ Int.* **49** 1907 (2009)
10. Nechaev Yu S *Phys. Usp.* **49** 563 (2006); *Usp. Fiz. Nauk* **176** 581 (2006)
11. Nechaev Yu S, Veziroglu T N *Int. J. Phys. Sci.* **10** (2) 54 (2015)
12. Nechaev Yu S et al. *Int. J. Hydrogen Energy* **45** 25030 (2020)
13. Nechaev Yu S et al. *Bull. Russ. Acad. Sci. Phys.* **85** 701 (2021); *Izv. Ross. Akad. Nauk Ser. Fiz.* **85** 918 (2021)
14. Zaika Yu V, Kostikova E K, Nechaev Yu S *Tech. Phys.* **66** 210 (2021); *Zh. Tekh. Fiz.* **91** 222 (2021)
15. Nechaev Yu S et al. *Fullerenes Nanotubes Carbon Nanostruct.* **28** 2147 (2020)
16. Nechaev Yu S et al. *J. Nucl. Mater.* **535** 152162 (2020)

17. Nechaev Yu S et al. *JETP Lett*. **114** 337 (2021); *Pis'ma Zh. Eksp. Teor. Fiz*. **114** 372 (2021)
18. Nechaev Yu S et al. *J. Surf. Invest. X-ray, Synchrotron Neutron Tech*. **16** 145 (2022); *Poverkhnost'. Rentgen. Sinkhrotron. Neitron. Issled*. (2) 64 (2022)
19. Nechaev Yu S et al. *Fullerenes Nanotubes Carbon Nanostruct*. **30** 211 (2022)
20. Nechaev Yu S et al. *Key Eng. Mater*. **910** 559 (2022)
21. Nechaev Yu S et al. *J. Carbon Res. C* **8** (1) 6 (2022)
22. Zhao X et al. *J. Chem. Phys*. **124** 194704 (2006)
23. Habenschaden E, Küppers J *Surf. Sci. Lett*. **138** L147 (1984)
24. Denisov E A, Kompaniets T N *Tech. Phys*. **46** 240 (2001); *Zh. Tekh. Fiz*. **71** (2) 111 (2001)
25. Zecho T et al. *J. Chem. Phys*. **117** 8486 (2002)
26. Zecho T, Güttler A, Küppers J *Carbon* **42** 609 (2004)
27. Hornekær L et al. *Phys. Rev. Lett*. **96** 156104 (2006)
28. Hornekær L et al. *Phys. Rev. Lett*. **97** 186102 (2006)
29. Rajasekaran S et al. *Phys. Rev. Lett*. **111** 085503 (2013)
30. Sofo J O, Chaudhari A S, Barber G D *Phys. Rev. B* **75** 153401 (2007)
31. Elias D C et al. *Science* **323** 610 (2009)
32. Sudan P et al. *Carbon* **41** 2377 (2003)
33. Nayyar I et al. *J. Carbon Res*. **6** 1 (2020)
34. Park C et al. *J. Phys. Chem. B* **103** 10572 (1999)
35. Baker R T K *Encyclopedia of Materials: Science and Technology* (Amsterdam: Elsevier, 2005)
36. Bashkin I O et al. *JETP Lett*. **79** 226 (2004); *Pis'ma Zh. Eksp. Teor. Fiz*. **79** 280 (2004)
37. Sun Y et al. *Sci. Adv*. **7** eabg3983 (2021)
38. Lee S-Y et al. *Processes* **10** 304 (2022)
39. Nechaev Yu S et al. *Kinet. Catal*. **63** 449 (2022); *Kinet. Kataliz* **63** 526 (2022)